

9. DATA REPORT: OXYGEN ISOTOPE STRATIGRAPHY OF ODP LEG 177 SITES 1088, 1089, 1090, 1093, AND 1094¹

David A. Hodell,² Christopher D. Charles,³ Jason H. Curtis,²
P. Graham Mortyn,^{3,4} Ulysses S. Ninnemann,^{3,5} and
Kathryn A. Venz²

INTRODUCTION

While onboard ship during Leg 177, we used variations in sediment physical properties (mainly percent color reflectance) in conjunction with biomagnetostratigraphy to correlate among sites and predict the position of marine isotope stages (MISs) (e.g., see fig. F11 in Shipboard Scientific Party, 1999, p. 45). Our working assumption was that physical properties of Leg 177 sediments are controlled mainly by variations in carbonate content. Previous studies of Southern Ocean sediment cores have shown that carbonate concentrations are relatively high during interglacial stages and low during glacial stages at sites located within the Polar Frontal Zone (PFZ). Today, the PFZ marks a lithologic boundary in underlying sediment separating calcareous oozes to the north and silica-rich facies to the south (Hays et al., 1976). Although there is debate whether the position of the “physical” PFZ actually moved during glacial-interglacial cycles (Charles and Fairbanks, 1990; Matsumoto et al., 2001), the “biochemical” PFZ, as expressed by the CaCO₃/opal boundary in sediments, certainly migrated north during glacials and south during interglacials. This gave rise to lithologic variations that are useful for stratigraphic correlation. At Leg 177 sites located north of the PFZ and at sublysoclinal depths, we expected the same pattern of carbonate variation because cores in the Atlantic basin are marked by increased carbonate dissolution during glacial periods and increased preservation during interglacials (Crowley, 1985).

¹Hodell, D.A., Charles, C.D., Curtis, J.H., Mortyn, P.G., Ninnemann, U.S., and Venz, K.A., 2003. Data report: Oxygen isotope stratigraphy of ODP Leg 177 Sites 1088, 1089, 1090, 1093, and 1094. In Gersonde, R., Hodell, D.A., and Blum, P. (Eds.), *Proc. ODP, Sci. Results*, 177, 1–26 [Online]. Available from World Wide Web: <http://www-odp.tamu.edu/publications/177_SR/VOLUME/CHAPTERS/SR177_09.PDF>. [Cited YYYY-MM-DD]

²Department of Geological Sciences, University of Florida, 241 Williamson Hall, PO Box 112120, Gainesville FL 32611, USA. Correspondence author: dhodell@geology.ufl.edu

³Geosciences Research Division, Scripps Institution of Oceanography, University of California, San Diego, La Jolla CA 92093, USA.

⁴Present address: Department of Earth and Environmental Sciences, California State University, Fresno, 2345 East San Ramon Avenue, Mail Stop MH-24, Fresno CA 93740, USA.

⁵Present address: Geologisk Institut, Universitetet i Bergen, Allegaten 41, N-5007 Bergen, Norway.

Since the end of Leg 177 in January 1998, we have analyzed stable isotopic ratios of foraminifers in thousands of samples from Ocean Drilling Program (ODP) Sites 1088, 1089, 1090, 1093, and 1094 (Fig. F1). These data provide a test of our preliminary shipboard stratigraphic interpretations. Here, we describe the methodology employed for stable isotope analysis and provide the resultant data. We present all oxygen isotope signals vs. meters composite depth (mcd) and compare them to variations in carbonate content or percent red reflectance (a proxy for carbonate content). For those records that are continuous enough to be correlated to oxygen isotope reference signals, we present the $\delta^{18}\text{O}$ signals vs. time. The paleoceanographic interpretations of the oxygen and carbon isotope results are presented in papers listed in the bibliography and several manuscripts in preparation.

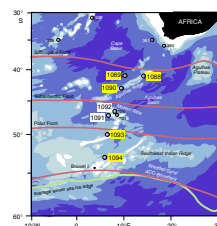
METHODS

Stable isotope analyses were conducted at the University of Florida (UF) and Scripps Institution of Oceanography (SIO). At UF, foraminifer tests were soaked in ~15% H_2O_2 for 30 min to remove organic matter. The tests were then rinsed with methanol and sonically cleaned to remove fine-grained particles. The methanol was removed with a syringe, and samples were dried in an oven at 50°C for 24 hr. The foraminifer calcite was loaded into individual reaction vessels, and each sample was reacted with three drops of H_3PO_4 (specific gravity = 1.92) using a Finnigan MAT Kiel III carbonate preparation device. Isotope ratios were measured online by a Finnigan MAT 252 mass spectrometer. Analytical precision was estimated by measuring eight standards (NBS-19) with each carousel containing 38 samples.

At SIO, foraminifer specimens were cleaned ultrasonically in distilled water until visually free of adhering particles and roasted under vacuum at 375°C for 1 hr to remove organic matter. Samples were then reacted in a common acid bath of H_3PO_4 using a Carousel-48 automatic carbonate preparation device. Isotope ratios of purified CO_2 gas were measured online with a Finnigan MAT 252 mass spectrometer. All isotope results are reported in standard delta notation relative to VPDB (Vienna PeeDee belemnite) (Coplen, 1996).

Analytical results from SIO and UF were intercalibrated by measuring a common set of benthic foraminiferal samples from Site 1089. For $\delta^{18}\text{O}$, UF results were systematically greater than those measured at SIO by ~0.4‰, whereas no offset was measured for $\delta^{13}\text{C}$. The intralaboratory $\delta^{18}\text{O}$ offset is large relative to the precision measured by repeated analysis of NBS-19. At UF, the long-term mean value of NBS-19 is $-2.13\text{\textperthousand} \pm 0.06\text{\textperthousand}$ for $\delta^{18}\text{O}$ and $1.93\text{\textperthousand} \pm 0.03\text{\textperthousand}$ for $\delta^{13}\text{C}$, slightly greater than the literature value of $-2.19\text{\textperthousand}$ for $\delta^{18}\text{O}$ but not large enough to account for the 0.4‰ offset. For several reasons, we don't believe the offset is due to differential treatment of samples for organic matter (chemical vs. roasting). Mead et al. (1993) found no significant differences between standards that were treated by both methods. Furthermore, *Cibicidoides* samples used for the intracalibration experiment were first cleaned at UF using the peroxide method and then sent to Scripps for analysis. We observe a similar offset in $\delta^{18}\text{O}$ for samples analyzed at UF using the PRISM mass spectrometer and ISOCARB (common acid bath) preparation device compared to the Finnigan MAT252/Kiel III system. The difference appears to be related to using a "common

F1. Location of Leg 177 drilling sites, p. 8.



acid bath" as opposed to a "single acid aliquot" device and may be dependent upon the reaction rate and how quickly the CO₂ is removed from the reaction vessel (equilibration with the H₂O and H₃PO₄). For consistency of isotopic results measured internally at UF and at SIO, we subtracted 0.4‰ from the UF δ¹⁸O data that were produced using the MAT252/Kiel III system.

Weight percent CaCO₃ was determined for Sites 1088, 1089, and 1090 at UF by coulometric titration with a UIC Inc. model 5240 total inorganic carbon (TIC) preparation system and model 5011 coulometer (Englemann et al., 1985). Analytical precision is estimated to be ±1% based on repeated analysis of reagent grade (100%) CaCO₃.

RESULTS

Site 1088

Site 1088 is located at 41°8.2'S, 13°33.8'E on the Agulhas Ridge in a water depth of 2082 m (Fig. F1). The upper 13.2 m of sediment in Hole 1088B (Cores 177-1088B-1H and 2H) was sampled every 5 cm, and the benthic foraminifer genus *Cibicidoides* was picked from the >150-μm size fraction for stable isotope analysis (Table T1). Despite relatively low sedimentation rates at Site 1088 in the Pleistocene (1 cm/k.y.), all isotope stages between MIS 1 and 31 are identifiable in the record (Fig. F2). The chronology for Site 1089 was developed by correlating the benthic δ¹⁸O record to the "low-latitude stack" of Bassinot et al. (1994) for the interval from 0 to 900 ka and to ODP Site 607 beyond 900 ka using the modified Site 607 timescale of Mix et al. (1995) (Fig. F3). The chronology of Bassinot et al. (1994) is virtually identical to SPECMAP (Imbrie et al., 1984) down to MIS 16, and it makes little difference whether the SPECMAP or the "low-latitude" stacks are used as the reference target for this interval. The Site 1088 isotope record is important because it provides a 1.1-m.y. history of the evolution of middepth waters in the South Atlantic (Hodell et al., 2003).

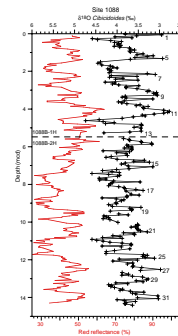
Site 1089

Site 1089 is located on a sediment drift in 4621 m of water in the southernmost Cape Basin, just north of the Agulhas Ridge at 40°56.2'S, 9°53.6'E (Fig. F1). Stable isotopes and weight percent CaCO₃ were measured on samples taken at 5-cm spacing from the modified Site 1089 composite section (Table T2) (Ninnemann et al., 1999; Hodell et al., 2001, in press; P.G. Mortyn et al., unpubl. data). The shipboard composite was modified slightly because oxygen isotope stratigraphy revealed that some of the shipboard splices overlapped slightly, whereas others were incomplete (Table T3). Sedimentation rates are high (average = 15 cm/k.y.) and provide an average sampling spacing of ~350 yr.

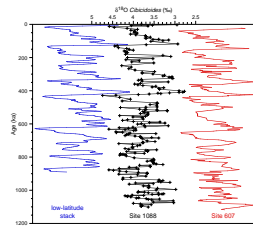
Specimens of the planktonic foraminifer *Globigerina bulloides* were selected from either the >250-μm (SIO data) or from the 212- to 300-μm (UF data) size fraction, and the benthic foraminifer *Cibicidoides* was analyzed from the >150-μm size fraction. Severe dissolution during peak interglacial conditions of MIS 9, 11, and 13 limits the continuity of the planktonic δ¹⁸O signal because tests of *G. bulloides* are poorly preserved in these intervals (Fig. F4). The benthic isotope record is near continuous except for part of MIS 7, where benthic foraminifers are very rare owing to dissolution.

T1. δ¹⁸O and δ¹³C for *Cibicidoides*, Site 1088, p. 20.

F2. *Cibicidoides* vs. red reflectance, Site 1088, p. 9.



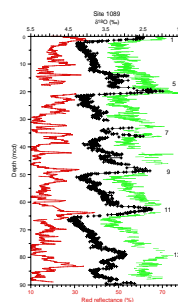
F3. Site 1088 benthic δ¹⁸O with Site 607 δ¹⁸O, p. 10.



T2. δ¹⁸O and δ¹³C for *Cibicidoides* and *G. bulloides*, Site 1089, p. 21.

T3. Site 1089 modified composite slice, p. 22.

F4. *Cibicidoides* and *G. bulloides* vs. red reflectance, Site 1089, p. 11.



The chronology for Site 1089 was developed by correlating the benthic $\delta^{18}\text{O}$ record to the SPECMAP reference signal (Fig. F5). For part of MIS 7, the planktonic $\delta^{18}\text{O}$ record was used for correlation to SPECMAP because of a break in the benthic signal. The Site 1089 benthic $\delta^{18}\text{O}$ record is remarkably similar to SPECMAP (Fig. F5), permitting the development of a precise orbitally tuned timescale for Site 1089.

The Site 1089 $\delta^{18}\text{O}$ record of *G. bulloides* is similar to deuterium isotope (δD) variations in the Vostok ice core (Petit et al., 1997) (Fig. F6), and millennial-scale oscillations have been used to correlate Vostok δD to the orbitally-tuned chronology of Site 1089 for the last 400 k.y. (Ninnemann et al., 1999; Mortyn et al., unpubl. data).

Site 1089 was the only Leg 177 site that did not follow the expected pattern of high-carbonate interglacials and low-carbonate glacials (Hodell et al., 2001), and, consequently, the shipboard prediction of stage placement in Site 1089 is incorrect. Carbonate variations at Site 1089 display a “Pacific-type” carbonate stratigraphy (Fig. F7) and, in fact, record changes in the saturation state of deepwater with much greater fidelity than Indo-Pacific records because of its high sedimentation rates (Hodell et al., 2001). Variations in weight percent carbonate lag the $\delta^{18}\text{O}$ signal by an average of 7.6 k.y. and are in phase with the rate of change (first derivative) of benthic $\delta^{18}\text{O}$. Peak carbonate preservation occurs during deglaciations (i.e., glacial terminations), whereas maximum dissolution occurs at the transition from interglacial to glacial periods.

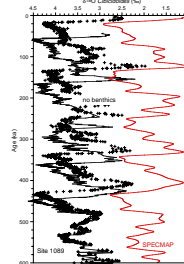
Site 1090

Site 1090 is also located on the Agulhas Ridge at 42°54.8'S, 8°54'E in a water depth of 3702 m (Fig. F1). A composite oxygen isotope record was developed at the location of ODP Site 1090 by splicing piston core TTN057-6-PC4 and Site 1090 at ~12.1 mcd (Fig. F8). The piston core was collected during the site survey cruise for Leg 177 and is at same position as Site 1090. The piston core has a complete record through MIS 12 (~440 ka) (Hodell et al., 2000) with sedimentation rates averaging 3 cm/k.y. The piston core was sampled at an interval of every 3 cm, yielding a temporal resolution of one sample every 1000 yr. The composite section of Site 1090 was sampled at 5-cm intervals (beginning at ~9 mcd to provide overlap with core TTN057-6), resulting in an average sampling frequency of one sample per 3 k.y. for the 2.8-m.y. record (Venz and Hodell, 2002). Sedimentation rates average ~3 cm/k.y. in the Pleistocene (0 to ~1.2 Ma), resulting in temporal resolution of one sample every 2 k.y. Prior to 1.2 Ma, sedimentation rates were lower (average = ~1.2 cm/k.y.) and yielded an average sampling frequency of one sample per 4 k.y.

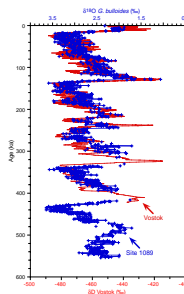
Stable isotopes were measured on the benthic foraminifer *Cibicidoides wuellerstorfi* and *Cibicidoides kullenbergi* as well as the planktonic foraminifer *Globigerina bulloides* (Table T4) (Hodell et al., 2000; Venz and Hodell, 2002). Tests of *Cibicidoides* were picked from the >212- μm size fraction, and one to three individuals were used for analysis. Specimens of *G. bulloides* were selected from the >212- to <300- μm size fraction, and eight to ten individuals were used for analysis.

For the last 450 k.y., the age model for the core TTN057-6/Site 1090 composite was derived by correlating the $\delta^{18}\text{O}$ signal to Site 607 using the modified timescale of Mix et al. (1995). The correlation of the core TTN057-6/Site 1090 oxygen isotopic record to the reference signals is

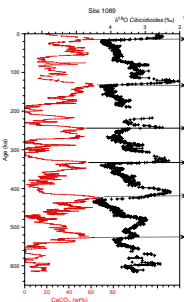
F5. SPECMAP correlation of Site 1089 benthic $\delta^{18}\text{O}$, p. 12.



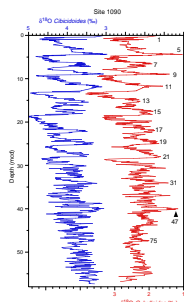
F6. SPECMAP comparison Site 1089 *G. bulloides* with Vostok ice core δD , p. 13.



F7. Carbonate and benthic $\delta^{18}\text{O}$, Site 1089, p. 14.



F8. *Cibicidoides* and *G. bulloides*, Site 1090, p. 15.



T4. $\delta^{18}\text{O}$ and $\delta^{13}\text{C}$ for foraminifers for Site 1090 and core TTN057-6, p. 23.

good at the stage level for the last 2 m.y. (Fig. F9), although brief hiatuses occur in the Pleistocene (Table T5). Correlation between ~2.0 and 2.9 Ma is less certain owing to low sedimentation rates, hiatuses, and the absence of *Cibicidoides* in some samples.

Site 1093

Site 1093 is located at ~49°59'S, 5°51.9'E near the present-day position of the Polar Front (Fig. F1). Initial hopes of obtaining a continuous isotope signal at this site were dashed by the scarcity of foraminifers during glacial periods. Benthic foraminifers were too scarce for analysis, so we focused on isotopic measurements of *Neogloboquadrina pachyderma* (sinistral) picked from the >150- μm size fraction (Table T6). Specimens of *N. pachyderma* are fairly abundant during interglacial periods but are rare or absent in glacial-aged sediments. Because of the discontinuous nature of the signal, we present the isotope data vs. meters composite depth only and have not correlated the signal to SPECMAP. Most low $\delta^{18}\text{O}$ values correspond to peaks in red reflectance (high carbonate content) during the earliest part of interglacial stages when sea-surface temperatures were greatest (Fig. F10). Interglacial stages are greatly expanded between MIS 1 and 15, whereas glacial stages are highly compressed. This pattern is caused by high biosiliceous productivity during interglacials when the Polar Front is near the site, as it is today, and low productivity during glacials when seasonal sea ice expanded northward and inhibited biological production.

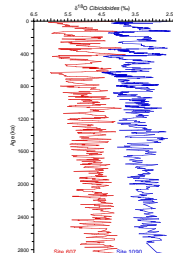
Site 1094

Site 1094 was the southernmost site drilled during Leg 177 and is located south of the Polar Front at 53.2°S, 5.1°E (Fig. F1). Specimens of *N. pachyderma* (sinistral) from the >150- μm fraction of the sediment were used for isotope analysis (Table T7) (Kanfoush et al., 2002). The abundance of planktonic foraminifers was variable at Site 1094, resulting in a discontinuous isotope record that includes gaps in late MIS 11 and 10, late MIS 7, and mid-late MIS 5 (Fig. F11). Variations in oxygen isotopes closely follow the percent red reflectance signal that is a proxy for carbonate content (Shipboard Scientific Party, 1999). The Site 1094 planktonic $\delta^{18}\text{O}$ signal has been correlated to the SPECMAP stack (Fig. F12), although the discontinuous nature of the record renders this correlation tentative.

ACKNOWLEDGMENTS

This research used samples and data provided by ODP. ODP is sponsored by the U.S. National Science Foundation (NSF) and participating countries under management of Joint Oceanographic Institutions, Inc. Funding for this research was provided by the U.S. Science Support Program and NSF Grants OCE-9907036 and OCE- 9910416 to D.A.H and C.D.C., respectively.

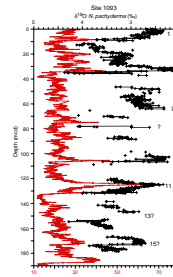
F9. Site 1090 benthic $\delta^{18}\text{O}$ vs. Site 607 benthic $\delta^{18}\text{O}$, p. 16.



T5. Missing isotope stages, Site 1090, p. 24.

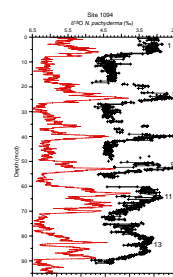
T6. $\delta^{18}\text{O}$ and $\delta^{13}\text{C}$ for *N. pachyderma*, Site 1093, p. 25.

F10. *N. pachyderma* vs. red reflectance, Site 1093, p. 17.

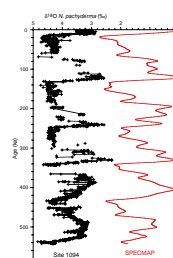


T7. $\delta^{18}\text{O}$ and $\delta^{13}\text{C}$ for *N. pachyderma*, Site 1094, p. 26.

F11. *N. pachyderma* vs. red reflectance, p. 18.



F12. SPECMAP *N. pachyderma* correlation, Site 1094, p. 19.



REFERENCES

- Bassinot, F.C., Labeyrie, L.D., Vincent, E., Quidelleur, X., Shackleton, N.J., and Lancelot, Y., 1994. The astronomical theory of climate and the age of the Brunhes-Matuyama magnetic reversal. *Earth Planet. Sci. Lett.*, 126:91–108.
- Charles, C.D., and Fairbanks, R.G., 1990. Glacial to interglacial changes in the isotopic gradients of Southern Ocean surface water. In Bleil, U., and Thiede, J. (Eds.), *Geological History of Polar Oceans: Arctic Versus Antarctic*: Netherlands (Kluwer Academic), 519–538.
- Coplen, T.B., 1996. Editorial: more uncertainty than necessary. *Paleoceanography*, 11:369–370.
- Crowley, T.J., 1985. Late Quaternary carbonate changes in the North Atlantic and Atlantic/Pacific comparisons. In Sundquist, E.T., and Broecker, W.S. (Eds.), *The Carbon Cycle and Atmospheric CO₂: Natural Variations, Archean to Present*. Geophys. Monogr., Am. Geophys. Union, 32:271–284.
- Engleman, E.E., Jackson, L.L., and Norton, D.R., 1985. Determination of carbonate carbon in geological materials by coulometric titration. *Chem. Geol.*, 53:125–128.
- Hays, J.D., Lozano, J.A., Shackleton, N.J., and Irving, G., 1976. Reconstruction of the Atlantic and western Indian Ocean sectors of the 18,000 B.P. Antarctic Ocean. In Cline, R.M., and Hays, J.D. (Eds.), *Investigations of Late Quaternary Paleoceanography and Paleoclimatology*. Mem.—Geol. Soc. Am., 145:337–372.
- Hodell, D.A., Charles, C.D., and Ninnemann, U.S., 2000. Comparison of interglacial stages in the South Atlantic sector of the southern ocean for the past 450 kyr: implications for Marine Isotope Stage (MIS) 11. *Global Planet. Change*, 24:7–26.
- Hodell, D.A., Venz, K.A., Charles, C.D., and Ninnemann, U.S., 2003. Pleistocene vertical carbon isotope and carbonate gradients in the South Atlantic sector of the Southern Ocean. *Geochem. Geophys. Geosyst.*, 4:10.1029/2002GC000367.
- Hodell, D.A., Charles, C.D., and Sierro, F.J., 2001. Late Pleistocene evolution of the ocean's carbonate system. *Earth Planet. Sci. Lett.*, 192:109–124.
- Hodell, D.A., Venz, K.A., Charles, C.D., and Sierro, F.J., in press. The mid-Brunhes transition in ODP sites 1089 and 1090. In Droxler, A. (Ed.), *Marine Isotope Stage 11: An Extreme Interglacial*. Geophys. Monogr., Am Geophys. Union.
- Imbrie, J., Hays, J.D., Martinson, D.G., McIntyre, A., Mix, A.C., Morley, J.J., Pisias, N.G., Prell, W.L., and Shackleton, N.J., 1984. The orbital theory of Pleistocene climate: support from a revised chronology of the marine δ¹⁸O record. In Berger, A., Imbrie, J., Hays, J., Kukla, G., and Saltzman, B. (Eds.), *Milankovitch and Climate* (Pt. 1), NATO ASI Ser. C, Math Phys. Sci., 126:269–305.
- Kanfoush, S.L., Hodell, D.A., Charles, C., and Janecek, T.R., 2002. Comparison of ice-rafted debris and physical properties in ODP Site 1094 (South Atlantic) with the Vostok ice core over the last three climate cycles. *Palaeogeogr., Palaeoclimatol., Palaeoecol.*, 182:329–349.
- Matsumoto, K., Lynch-Stieglitz, and Anderson, R.F., 2001. Similar glacial and Holocene Southern Ocean hydrography. *Paleoceanography*, 16:445–454.
- Mead, G.A., Hodell, D.A., and Ciecielski, P.F., 1993. Late Eocene to Oligocene vertical isotopic gradients in the South Atlantic: implications for warm saline deep water. In Kennett, J.P., and Warnke, D. (Eds.), *The Antarctic Paleoenvironment: A Perspective on Global Change*. Am. Geophys. Union, Antarc. Res. Ser., 60:27–48.
- Mix, A.C., Pisias, N.G., Rugh, W., Wilson, J., Morey, A., and Hagelberg, T.K., 1995. Benthic foraminifer stable isotope record from Site 849 (0–5 Ma): local and global climate changes. In Pisias, N.G., Mayer, L.A., Janecek, T.R., Palmer-Julson, A., and van Andel, T.H. (Eds.), *Proc. ODP, Sci. Results*, 138: College Station, TX (Ocean Drilling Program), 371–412.
- Ninnemann, U.S., Charles, C.D., and Hodell, D.A., 1999. Origin of global millennial-scale climate events: constraints from the southern ocean deep-sea sedimentary record. In Clark, P.U., Webb, R.S., Keigwin, L.D. (Eds.), *Mechanisms of Global Cli-*

- mate Change at Millennial Time Scales.* Geophys. Monogr., Am. Geophys. Union, 112:99–112.
- Petit, J.R., Basile, I., Leruyuet, A., Raynaud, D., Lorius, C., Jouzel, J., Stievenard, M., Lipenkov, V.Y., Barkov, N.I., Kudryashov, B.-B., Davis, M., Saltzman, E., and Kotlyakov, V., 1997. Four climatic cycles in Vostok ice core. *Nature*, 387:121–164.
- Shipboard Scientific Party, 1999. Leg 177 summary: Southern Ocean paleoceanography. In Gersonde, R., Hodell, D.A., Blum, P., et al., *Proc. ODP Init. Repts.*, 177: College Station, TX (Ocean Drilling Program), 1–67.
- Venz, K.A., and Hodell, D.A., 2002. Plio-Pleistocene record of deep-water circulation in the Southern Ocean from ODP Leg 177, Site 1090. *Palaeogeogr., Palaeoclimatol., Palaeoecol.*, 182:197–220.

Figure F1. Location of Leg 177 drilling sites in the South Atlantic relative to major frontal boundaries. Oxygen isotope records are presented here for those sites designated in yellow.

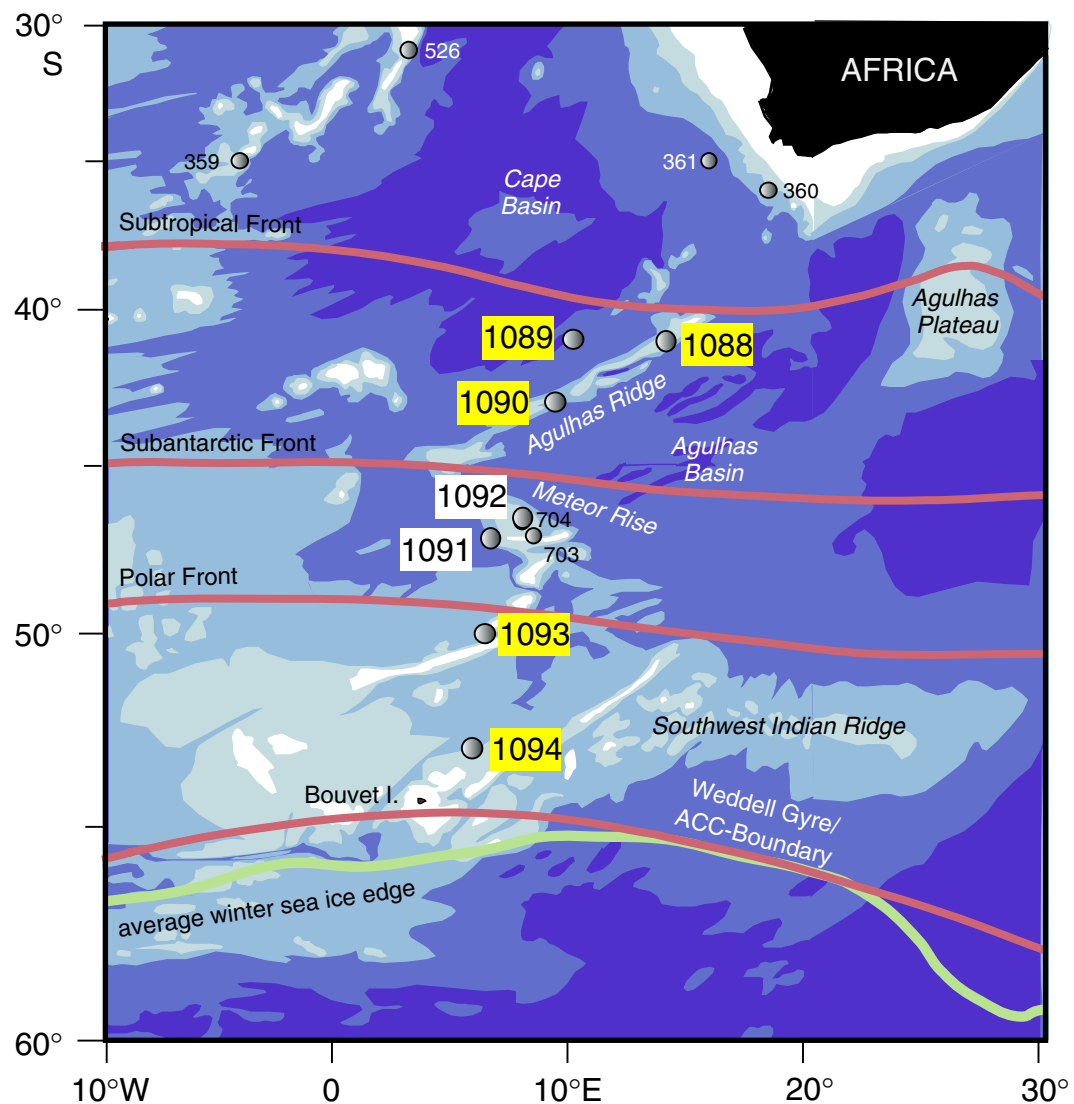


Figure F2. Oxygen isotope results for the benthic foraminifer *Cibicidoides* (black line) at Site 1088 relative to percent red reflectance (650–750 nm; red line) measured during Leg 177 (Shipboard Scientific Party, 1999). All isotopic stages from MIS 1 to 31 are identified in the upper 14.5 mcd corresponding to Cores 177-1088B-1H and 2H.

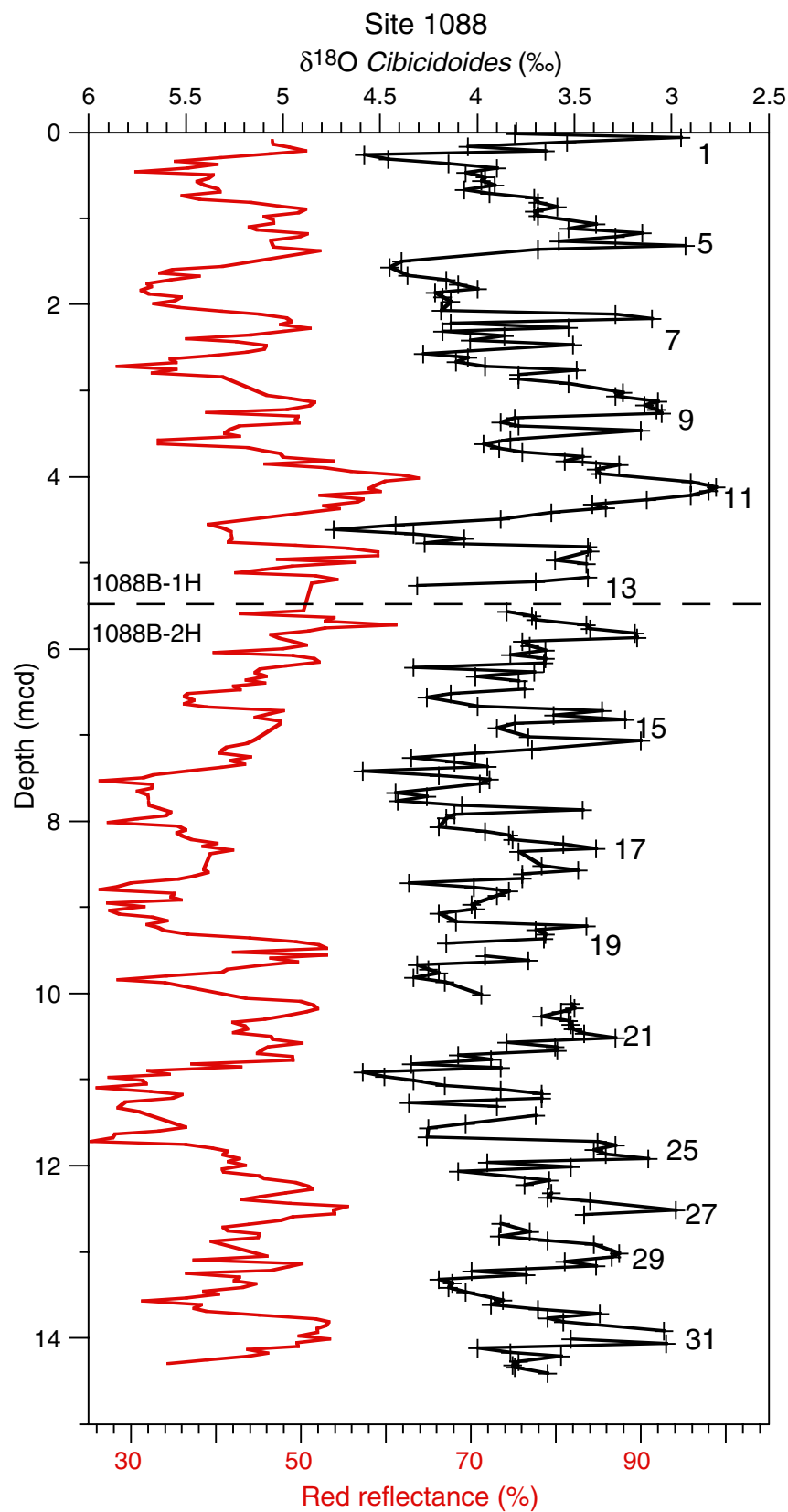


Figure F3. Correlation of Site 1088 benthic $\delta^{18}\text{O}$ (black line) to the “low-latitude” stack (blue line) of Bassinot et al. (1994) and the benthic $\delta^{18}\text{O}$ signal of Site 607 (red line) using the modified timescale of Mix et al. (1995).

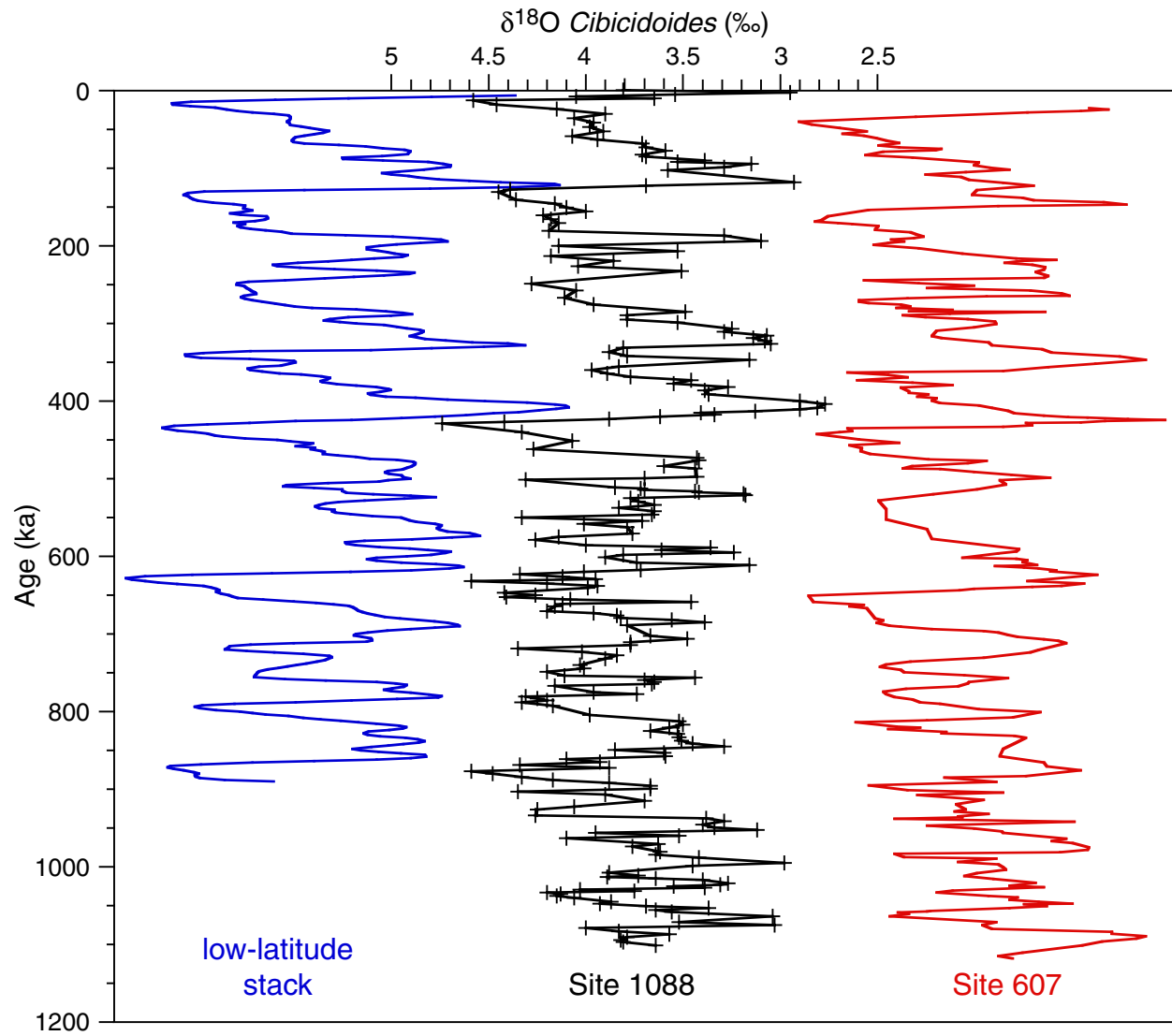


Figure F4. Oxygen isotope results for the benthic foraminifer *Cibicidoides* (black line) and planktonic foraminifer *Globigerina bulloides* (green line) at Site 1089 relative to percent red reflectance (650–750 nm; red line) measured during Leg 177 (Shipboard Scientific Party, 1999).

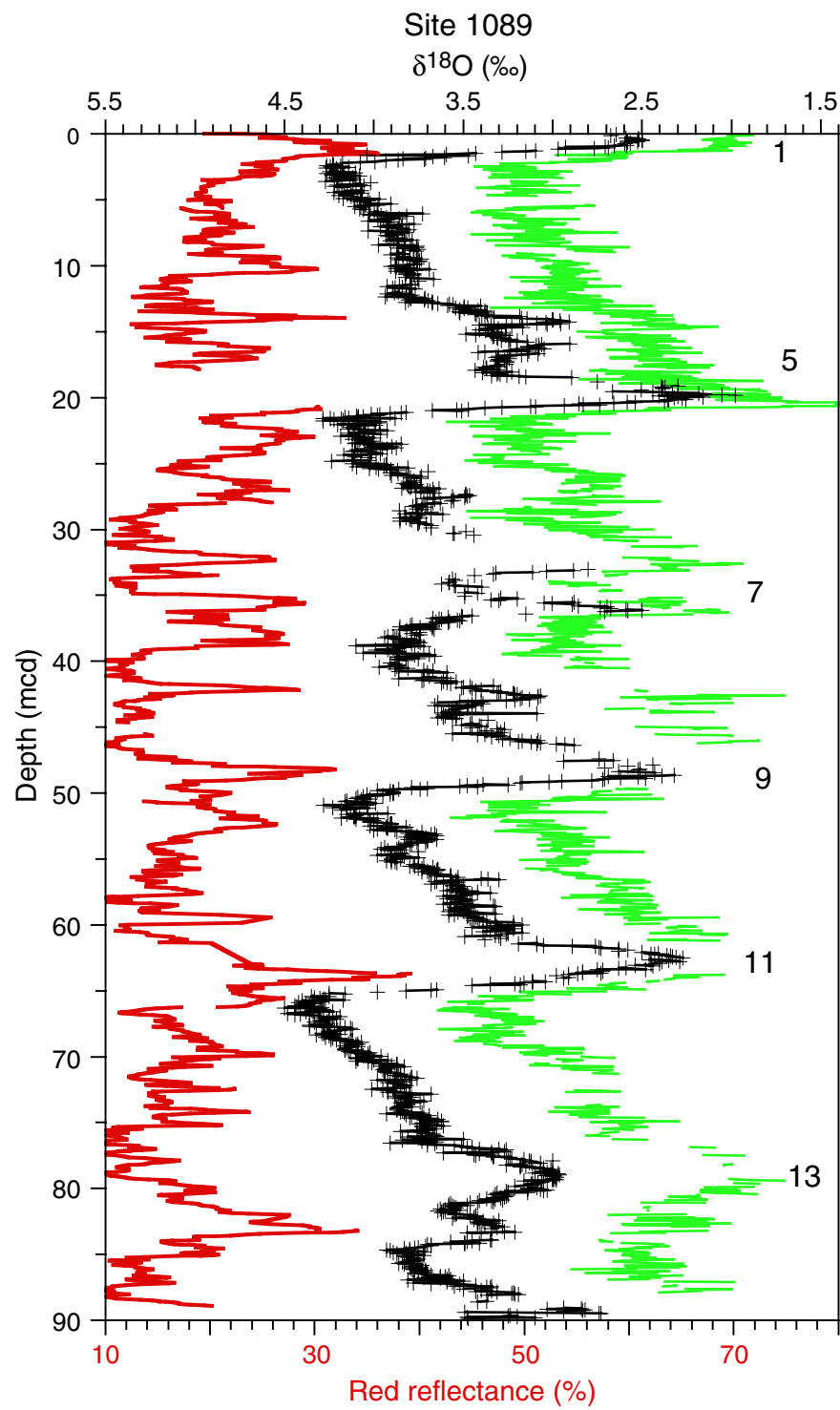


Figure F5. Correlation of Site 1089 benthic $\delta^{18}\text{O}$ (black line) to the SPECMAP stack (red line) of Imbrie et al. (1984).

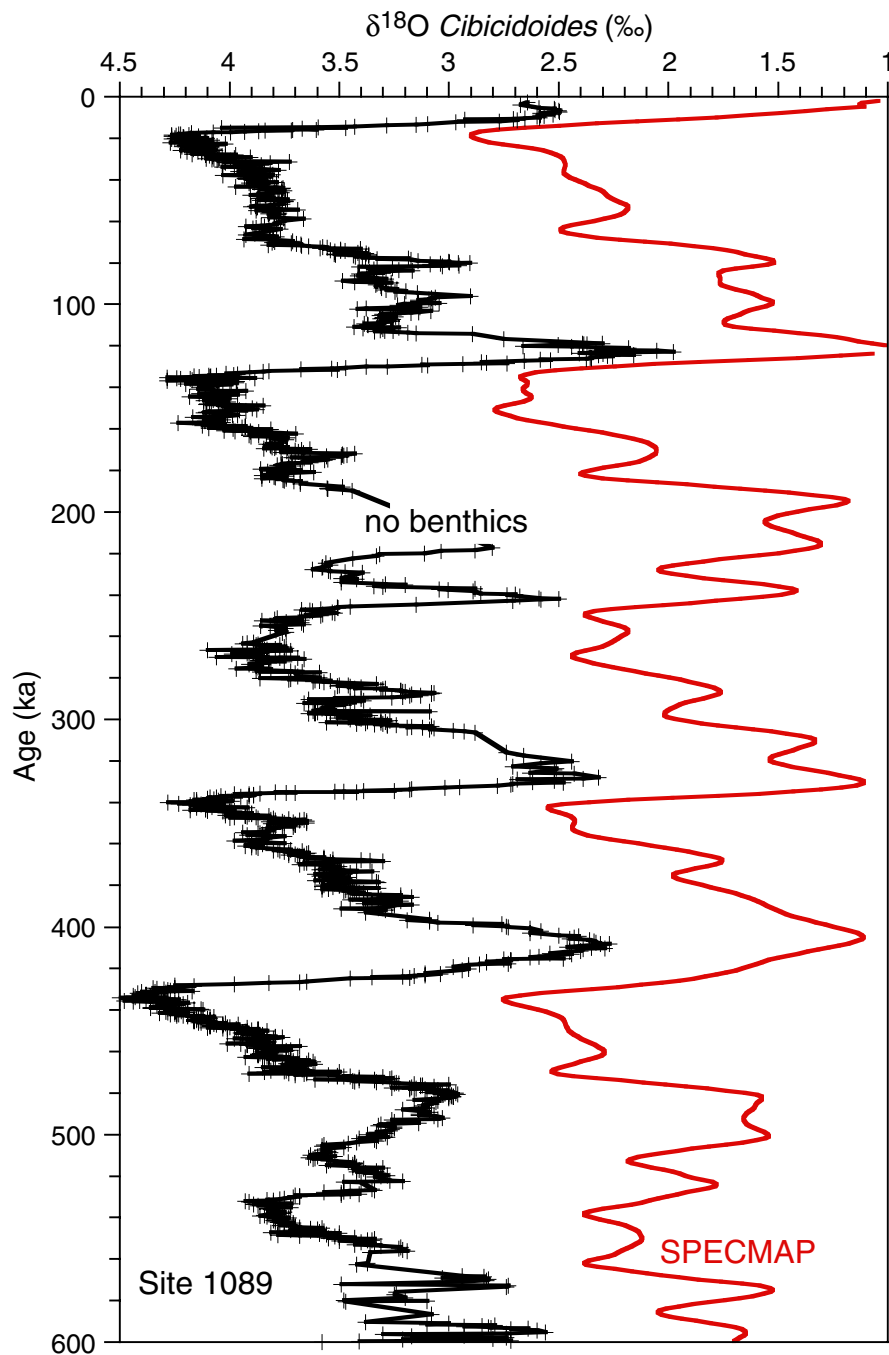


Figure F6. Comparison of the Site 1089 $\delta^{18}\text{O}$ record of *G. bulloides* (blue line) on the SPECMAP timescale with the δD signal (red line) from the Vostok ice core on the GT4 timescale (Petit et al., 1997).

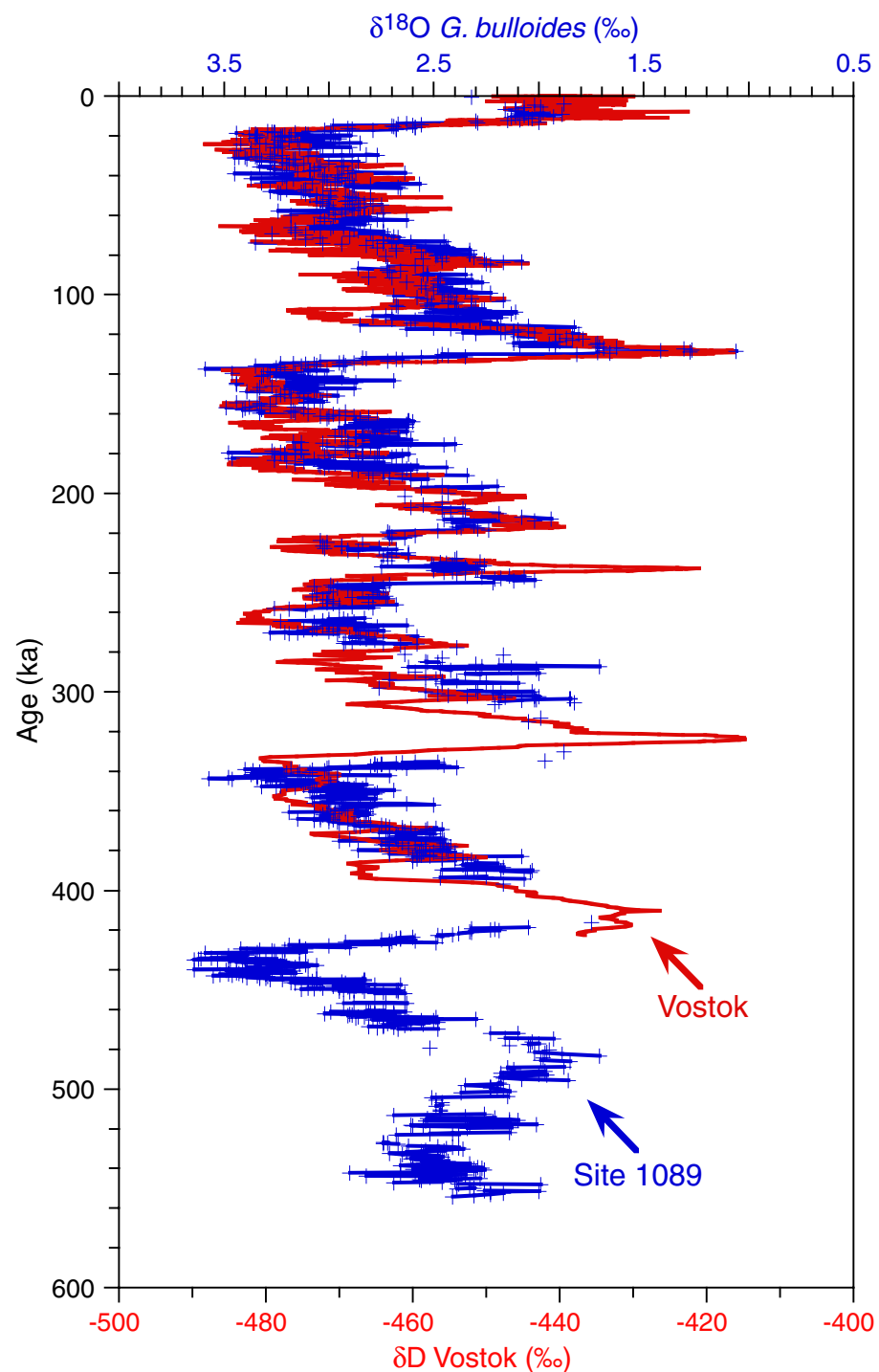


Figure F7. Carbonate (red line) and benthic $\delta^{18}\text{O}$ signals (black line) from Site 1089. Glacial terminations are marked by roman numerals and correspond to peaks in weight percent carbonate.

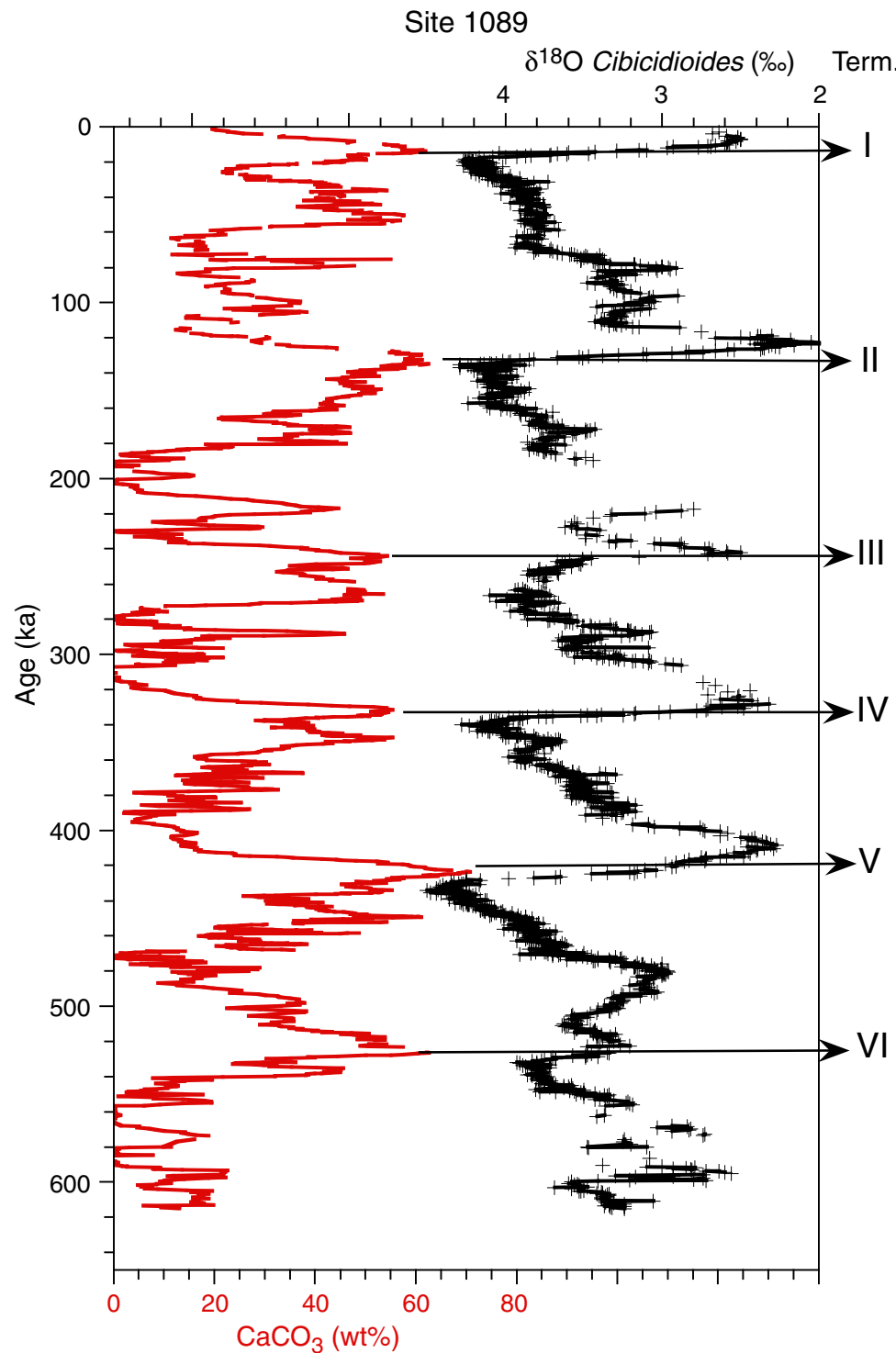


Figure F8. Oxygen isotope results for the benthic foraminifer *Cibicidoides* (blue line) and planktonic foraminifer *G. bulloides* (red line) at Site 1090.

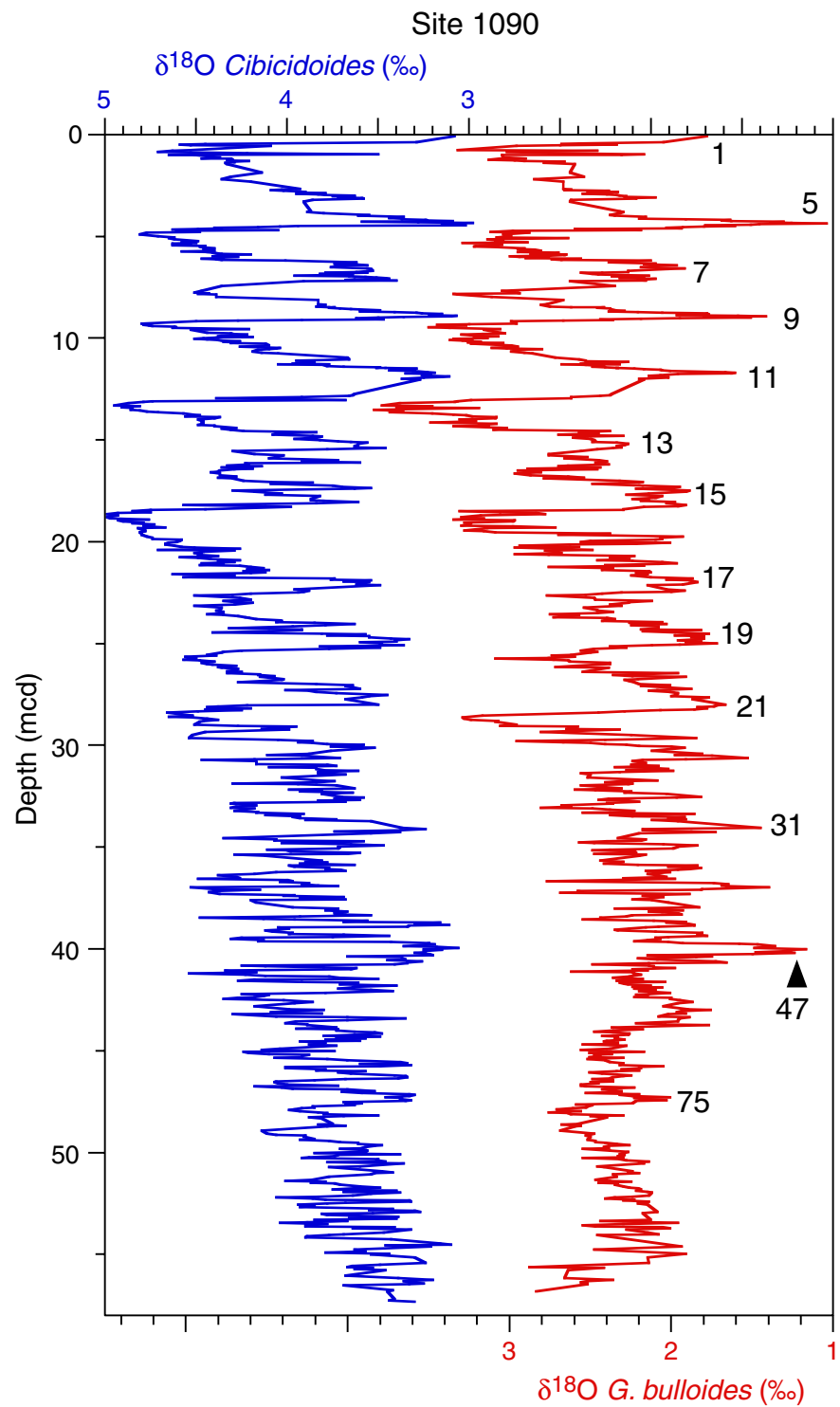


Figure F9. Correlation of benthic $\delta^{18}\text{O}$ (blue line) at Site 1088 to the benthic $\delta^{18}\text{O}$ signal of Site 607 (red line) using the modified timescale of Mix et al. (1995).

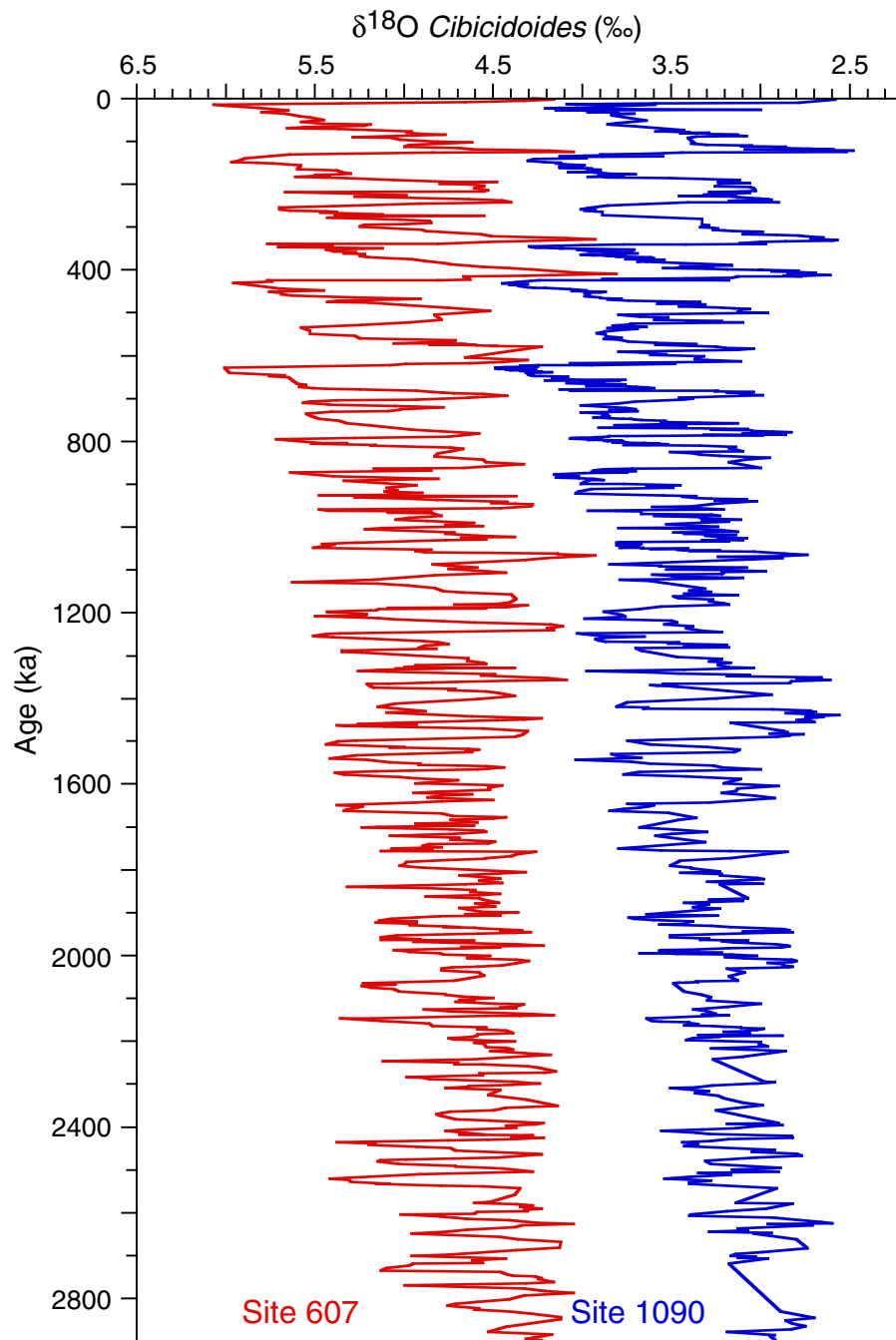


Figure F10. Oxygen isotope results for the planktonic foraminifer *N. pachyderma* (black line) at Site 1093 relative to percent red reflectance (650–750 nm; red line) measured during Leg 177 (Shipboard Scientific Party, 1999).

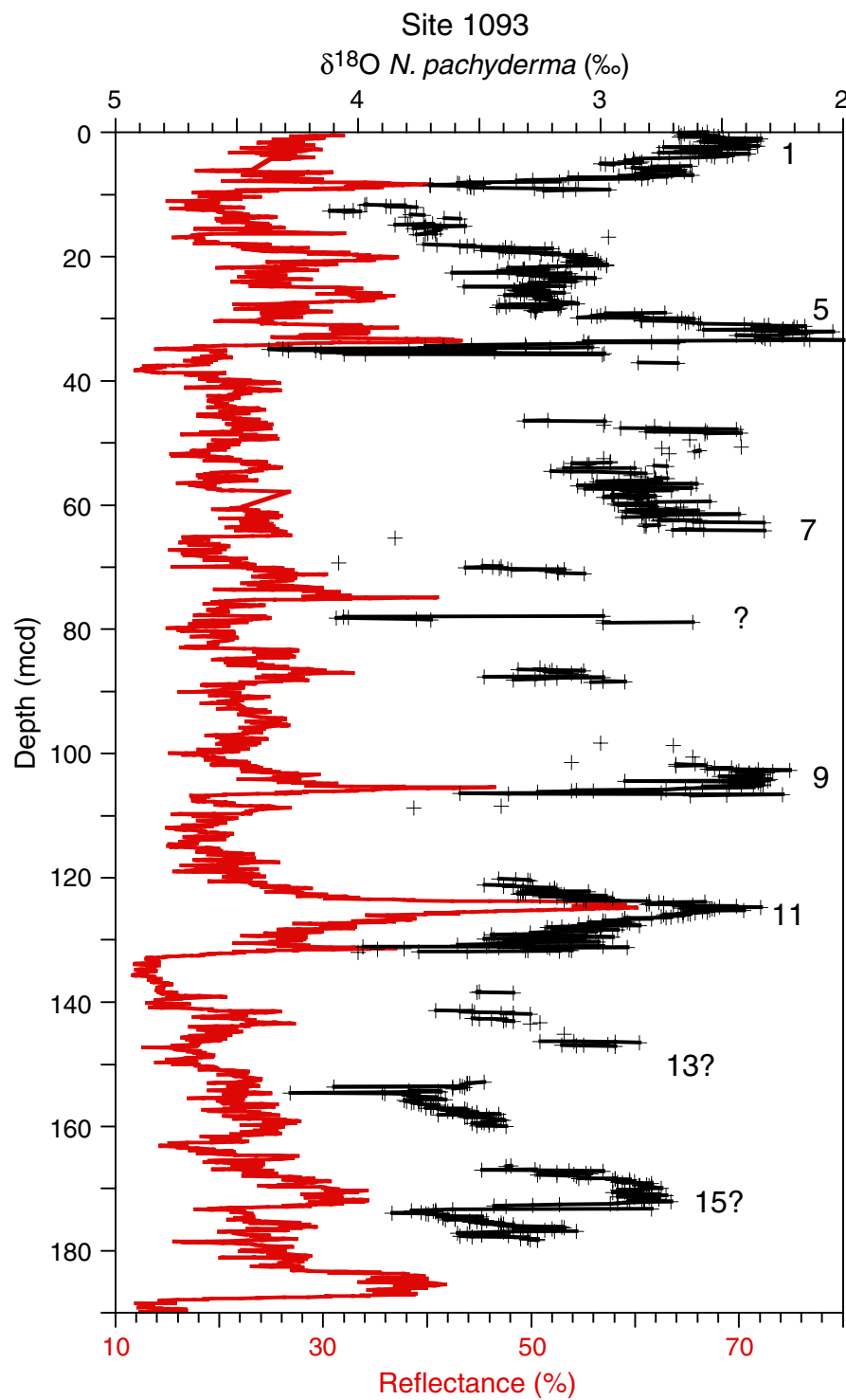


Figure F11. Oxygen isotope results for the planktonic foraminifer *N. pachyderma* (black line) in Site 1094 relative to percent red reflectance (650–750 nm; red line) measured during Leg 177 (Shipboard Scientific Party, 1999).

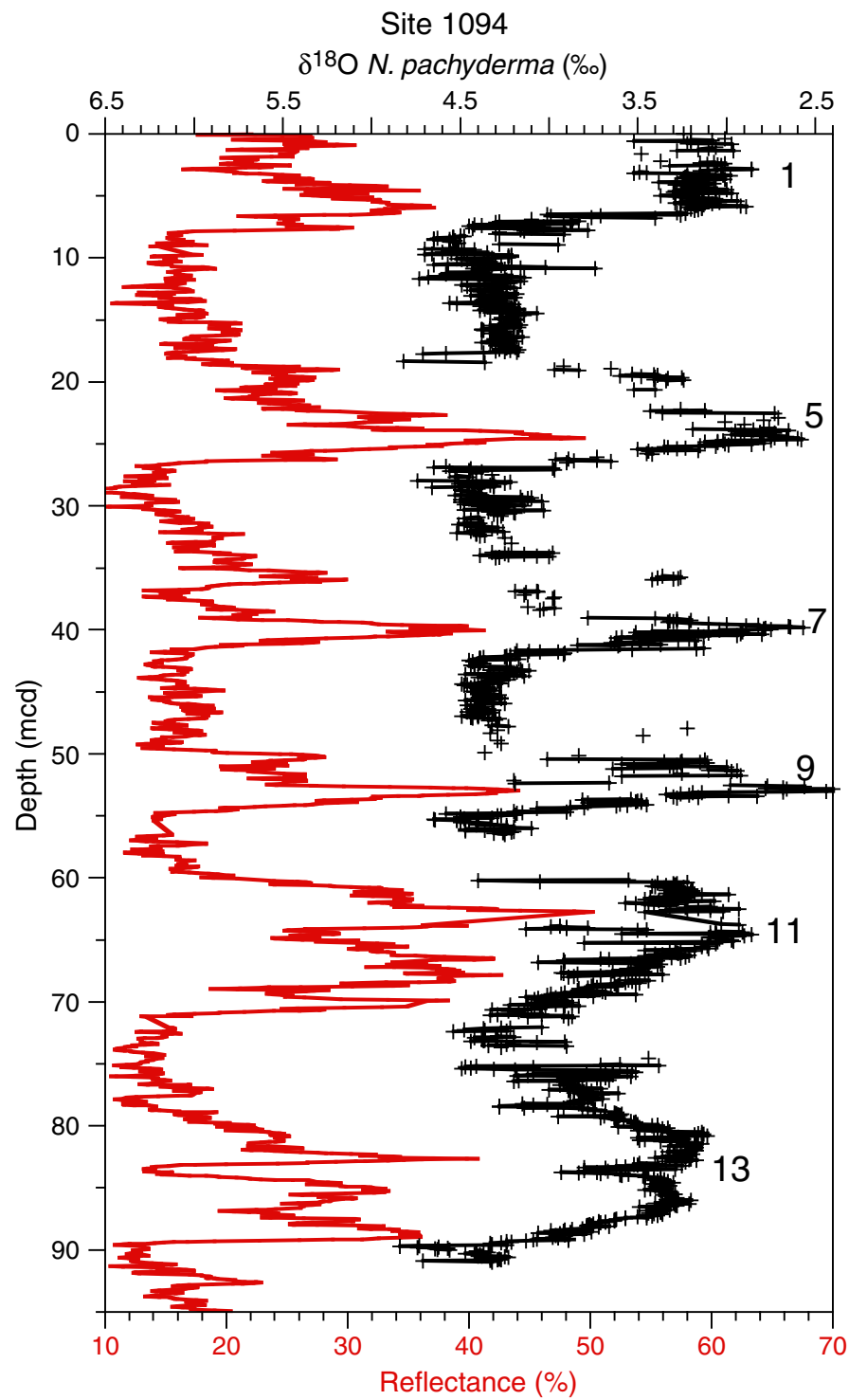


Figure F12. Correlation of the Site 1094 planktonic $\delta^{18}\text{O}$ signal of *N. pachyderma* (black line) to the SPEC-MAP stack (red line) of Imbrie et al. (1984).

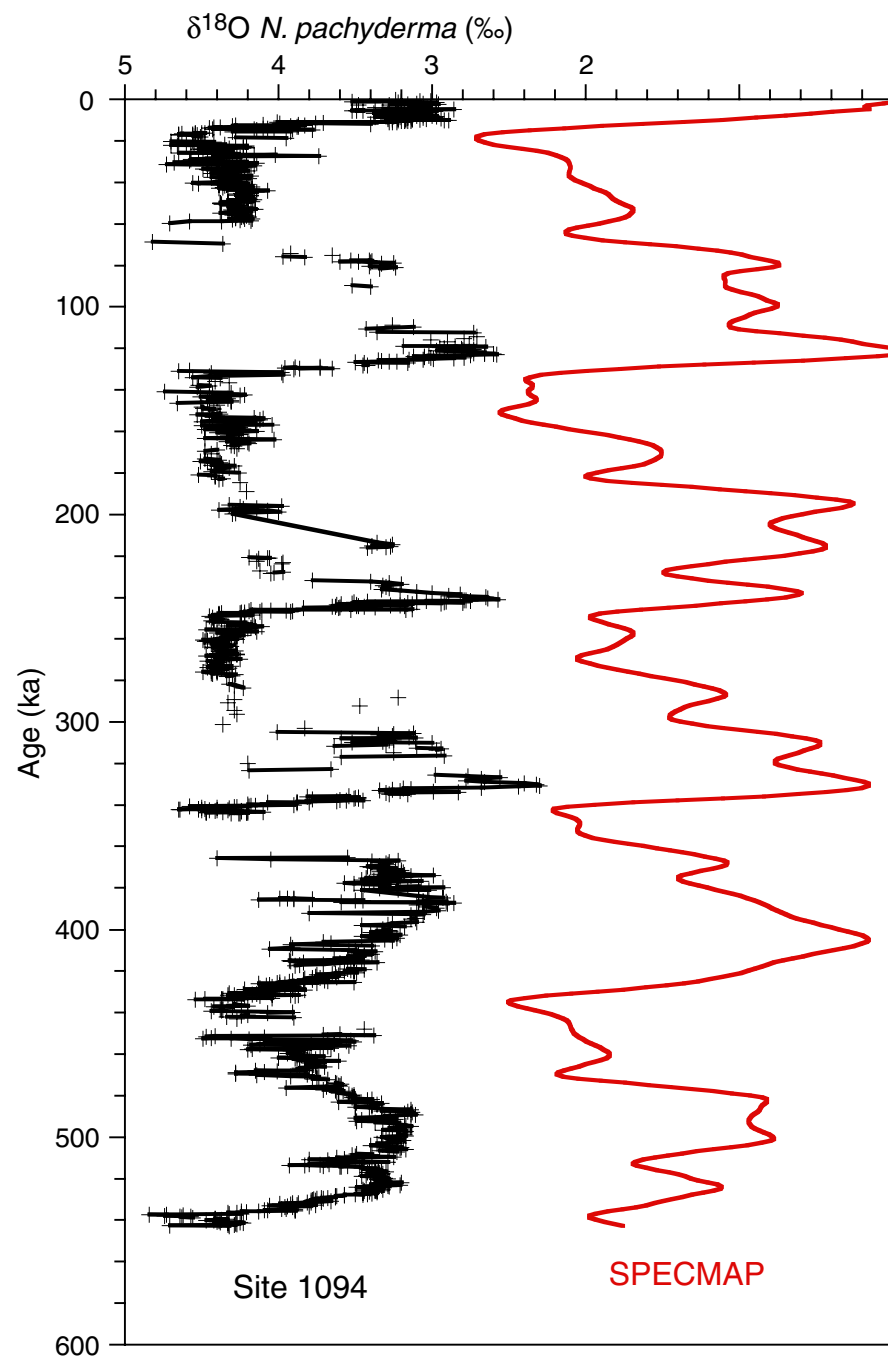


Table T1. $\delta^{18}\text{O}$ and $\delta^{13}\text{C}$ for the benthic foraminifer *Cibicidoides* at ODP Site 1088 and weight percent CaCO_3 of the sediment.

Site	Hole	Core	Section	Interval top (cm)	Interval bottom (cm)	Depth (mcd)	Age (ka)	$\delta^{18}\text{O}$ (‰)	$\delta^{13}\text{C}$ (‰)	CaCO_3 (wt%)	Lab
1088	B	1	1	2	4	0.02	3.33	3.81	0.55	90.64	UF
1088	B	1	1	7	9	0.07	5.87	2.95	0.44	86.35	UF
1088	B	1	1	12	14	0.12	8.40	3.54	0.53	89.80	UF
1088	B	1	1	17	19	0.17	10.93	4.05	0.09	87.53	UF
1088	B	1	1	22	24	0.22	13.47	3.65	0.52	89.34	UF
1088	B	1	1	27	29	0.27	16.00	4.58	0.28	86.39	UF
1088	B	1	1	32	34	0.32	21.75	4.46	0.28	77.75	UF
1088	B	1	1	37	39	0.37	27.50	4.15	0.44	83.55	UF
1088	B	1	1	42	44	0.42	33.25	3.90	0.38	81.51	UF
1088	B	1	1	47	49	0.47	39.00	4.06	0.44	88.77	UF
1088	B	1	1	52	54	0.52	44.75	3.96	0.54	83.97	UF
1088	B	1	1	57	59	0.57	50.50	3.98	0.51	87.03	UF
1088	B	1	1	62	64	0.62	56.25	3.91	0.33	85.68	UF
1088	B	1	1	67	69	0.67	62.00	4.07	0.16	87.09	UF
1088	B	1	1	72	74	0.72	66.80	3.94	0.72	86.07	UF
1088	B	1	1	77	79	0.77	71.60	3.71	0.74	88.81	UF
1088	B	1	1	82	84	0.82	76.40	3.69	0.57	86.76	UF
1088	B	1	1	87	89	0.87	81.20	3.59	0.65	89.48	UF
1088	B	1	1	92	94	0.92	86.00	3.71	0.42	90.44	UF
1088	B	1	1	97	99	0.97	88.40	3.69	0.66	88.02	UF
1088	B	1	1	107	109	1.07	93.20	3.39	0.60	88.01	UF
1088	B	1	1	112	114	1.12	95.60	3.53	0.55	86.16	UF
1088	B	1	1	117	119	1.17	98.00	3.15	0.49	86.08	UF
1088	B	1	1	122	124	1.22	102.00	3.29	0.37	87.27	UF
1088	B	1	1	127	129	1.27	106.00	3.58	0.67	84.40	UF
1088	B	1	1	132	134	1.32	121.45	2.93	0.44	86.58	UF
1088	B	1	1	137	139	1.37	126.00	3.69	0.11	87.38	UF
1088	B	1	2	0	2	1.50	131.20	4.39	0.00	86.85	UF
1088	B	1	2	7	9	1.57	134.00	4.45	0.05	85.79	UF
1088	B	1	2	17	19	1.67	144.00	4.36	-0.08	85.01	UF
1088	B	1	2	22	24	1.72	149.00	4.16	-0.10	84.98	UF
1088	B	1	2	27	29	1.77	154.00	4.10	-0.06	85.28	UF
1088	B	1	2	32	34	1.82	159.00	4.00	0.19	84.84	UF
1088	B	1	2	37	39	1.87	164.00	4.22	0.18	86.96	UF
1088	B	1	2	42	44	1.92	169.00	4.18	0.20	89.53	UF
1088	B	1	2	47	49	1.97	174.00	4.14	-0.10	86.05	UF
1088	B	1	2	57	59	2.07	184.00	4.19	-0.05	85.66	UF
1088	B	1	2	62	64	2.12	190.50	3.29	0.38	87.61	UF
1088	B	1	2	67	69	2.17	197.00	3.10	0.48	86.84	UF
1088	B	1	2	72	74	2.22	203.50	4.14	0.21	90.52	UF
1088	B	1	2	77	79	2.27	210.00	3.53	0.11	90.78	UF
1088	B	1	2	82	84	2.32	216.50	4.18	0.26	86.54	UF
1088	B	1	2	87	89	2.37	223.00	3.86	0.42	90.91	UF
1088	B	1	2	92	94	2.42	229.50	4.04	0.16	89.88	UF
1088	B	1	2	97	99	2.47	236.00	3.51	0.18	87.02	UF
1088	B	1	2	107	109	2.57	251.84	4.28	0.09	85.60	UF
1088	B	1	2	112	114	2.62	260.88	4.05	-0.02	85.24	UF
1088	B	1	2	117	119	2.67	269.92	4.11	0.00	82.18	UF
1088	B	1	2	122	124	2.72	278.96	3.96	0.22	87.23	UF
1088	B	1	2	127	129	2.77	288.00	3.49	0.28	88.44	UF
1088	B	1	2	132	134	2.82	293.00	3.79	0.41	85.47	UF
1088	B	1	2	137	139	2.87	298.00	3.79	0.45	89.60	UF
1088	B	1	2	142	144	2.92	301.95	3.53	0.27	88.23	UF
1088	B	1	3	2	4	3.02	309.85	3.25	0.40	81.13	UF
1088	B	1	3	7	9	3.07	313.80	3.29	0.38	89.47	UF
1088	B	1	3	13	15	3.13	318.54	3.07	0.21	90.41	UF
1088	B	1	3	17	19	3.17	321.70	3.14	-0.25	87.54	UF
1088	B	1	3	22	24	3.22	325.65	3.08	0.21	89.65	UF
1088	B	1	3	27	29	3.27	329.60	3.05	0.17	86.91	UF
1088	B	1	3	32	34	3.32	334.70	3.81	0.15	89.68	UF
1088	B	1	3	37	39	3.37	339.80	3.88	0.22	90.49	UF
1088	B	1	3	42	44	3.42	344.90	3.79	-0.17	88.56	UF
1088	B	1	3	47	49	3.47	350.00	3.16	-0.06	89.64	UF
1088	B	1	3	57	59	3.57	358.79	3.83	-0.21	87.29	UF

Note: Only a portion of this table appears here. The entire table is available in [ASCII format](#).

Table T2. $\delta^{18}\text{O}$ and $\delta^{13}\text{C}$ for the benthic foraminifer *Cibicidoides* and planktonic foraminifer *G. bulloides* at Site 1089, weight percent CaCO_3 , and percent fragmentation of planktonic foraminifers.

Site	Hole	Core	Section	Interval top (cm)	Interval bottom (cm)	Depth (modified mcd)	Age (ka)	$\delta^{18}\text{O}$ <i>G. bulloides</i> (‰)	$\delta^{13}\text{C}$ <i>G. bulloides</i> (‰)	$\delta^{18}\text{O}$ <i>Cibicidoides</i> (‰)	$\delta^{13}\text{C}$ <i>Cibicidoides</i> (‰)	Lab	CaCO_3 (wt%)	fragmentation (%)	Lab
1089	A	1	1	0	1.5	-0.24	0.00					SIO			UF
1089	A	1	1	5	6.5	-0.19	0.55	2.32	1.48			SIO		88.2	UF
1089	A	1	1	10	11.5	-0.14	1.04					SIO	20.0	89.3	UF
1089	A	1	1	15	16.5	-0.09	1.49					SIO	19.6	91.2	UF
1089	A	1	1	20	21.5	-0.04	1.99					SIO	20.4	88.4	UF
1089	A	1	1	25	26.5	0.01	2.48					SIO	22.7	87.4	UF
1089	A	1	1	30	31.5	0.06	2.98			2.64	0.20	SIO	22.6	78.6	UF
1089	A	1	1	35	36.5	0.11	3.48					SIO	24.0	92.7	UF
1089	A	1	1	40	41.5	0.16	3.98	1.88	1.13	2.68	0.48	SIO	25.7	74.0	UF
1089	A	1	1	45	46.5	0.21	4.47	2.02	1.28			SIO	29.3	82.9	UF
1089	A	1	1	50	51.5	0.26	4.97					SIO			UF
1089	A	1	1	55	56.5	0.32	5.52	1.99	1.05	2.59	0.31	SIO	33.8	70.2	UF
1089	A	1	1	58.5	60	0.36	5.96	2.07	1.22	2.52	0.27	SIO	32.8	78.8	UF
1089	A	1	1	65	66.5	0.41	6.46	2.11	1.32	2.52	0.15	SIO	37.9	77.8	UF
1089	A	1	1	70	71.5	0.46	6.96	2.16	1.15	2.50	0.26	SIO	38.8	72.1	UF
1089	A	1	1	74	75.5	0.51	7.45	2.11	1.22	2.50	0.30	SIO	42.4	71.1	UF
1089	A	1	1	80	82	0.56	7.95	1.98	1.08	2.58	0.18	SIO	45.8	61.0	UF
1089	A	1	1	85	86.5	0.61	8.45	2.07	1.19	2.53	0.25	SIO	47.7	60.6	UF
1089	A	1	1	90	91.5	0.66	8.95	2.10	0.89	2.58	-0.04	SIO	46.3	56.2	UF
1089	A	1	1	95	96.5	0.73	9.41	1.89	1.01	2.57	0.37	SIO	46.4	67.8	UF
1089	A	1	1	100	101.5	0.76	9.63	1.99	0.91	2.60	0.42	SIO			UF
1089	A	1	1	105	106.5	0.82	9.98	2.07	1.04			SIO	53.6	58.0	UF
1089	A	1	1	110	111.5	0.86	10.27	2.11	0.93	2.59	0.11	SIO	54.1	50.9	UF
1089	A	1	1	115	116.5	0.91	10.59	1.93	0.63	2.66	-0.07	SIO	56.4	49.2	UF
1089	A	1	1	120	121.5	0.96	10.91	2.13	0.57	2.71	-0.36	SIO	55.3	48.0	UF
1089	A	1	1	125	126.5	1.01	11.22	2.05	0.61	2.93	-0.06	SIO	57.0	47.8	UF
1089	A	1	1	130	131.5	1.06	11.54	2.03	0.49	2.69	-0.13	SIO	57.8	40.3	UF
1089	A	1	1	135	136.5	1.11	11.86	2.09	0.56	2.77	0.15	SIO	57.0	40.6	UF
1089	A	1	1	140	141.5	1.16	12.18	2.15	0.43	2.97	-0.14	SIO	57.8	34.0	UF
1089	A	1	1	145	146.5	1.21	12.49	2.15	0.57			SIO		21.3	UF
1089	A	1	2	0	1.5	1.26	12.81	2.30	0.33			SIO			UF
1089	A	1	2	5	6.5	1.32	13.16	2.00	0.04	3.10	0.02	SIO	57.2	23.9	UF
1089	A	1	2	10	11.5	1.37	13.48	2.29	-0.01	3.15	0.07	SIO	61.3	35.0	UF
1089	A	1	2	15	16.5	1.41	13.77	2.63	0.20	3.29	0.14	SIO	60.4	28.4	UF
1089	A	1	2	20	21.5	1.46	14.08	2.67	0.40			SIO	61.8	23.8	UF
1089	A	1	2	25	26.5	1.50	14.34	2.56	-0.07	3.43	0.01	SIO	61.1	25.0	UF
1089	A	1	2	30	31.5	1.57	14.75	2.60	0.06	3.60	-0.37	SIO	59.6	19.5	UF
1089	A	1	2	35	36.5	1.61	15.00	2.98	0.09	4.04	-0.59	SIO	58.8	47.1	UF
1089	A	1	2	40	41.5	1.66	15.21	2.70	0.21	3.47	-0.57	SIO	55.5	14.5	UF
1089	A	1	2	45	46.5	1.71	15.43	2.69	0.00	3.67	-0.21	SIO	52.3	17.7	UF
1089	A	1	2	50	51.5	1.76	15.65	2.59	-0.01			SIO			UF
1089	A	1	2	55	56.5	1.82	15.89			3.61	-0.32	SIO	48.6	39.1	UF
1089	A	1	2	59	61	1.86	16.08	2.59	-0.18	3.71	-0.49	SIO	50.4	58.7	UF
1089	A	1	2	65	66.5	1.91	16.30	2.68	-0.01	3.84	-0.86	SIO	46.5	41.7	UF
1089	A	1	2	70	71.5	1.95	16.47	2.91	-0.15	3.72	-0.43	SIO	48.8	66.9	UF

Note: Only a portion of this table appears here. The entire table is available in [ASCII format](#).

Table T3. Modified composite splice, at Site 1089.

Core, section, interval	Depth (mbsf)	Depth (revised mcd)		Core, section, interval	Depth (mbsf)	Depth (revised mcd)
177-						
1089A-1H-1, 0	0	-0.24	Tie to	1089A-1H-4, 135	5.85	5.61
1089D-2H-2, 35	8.55	5.67	Tie to	1089D-2H-5, 130	14	11.12
1089A-2H-3, 130	11.6	11.18	Tie to	1089A-2H-5, 110	14.4	13.98
1089B-2H-3, 55	8.35	14.05	Tie to	1089B-2H-6, 50	12.9	18.5
1089D-3H-4, 115	18.51	18.53	Tie to	1089D-3H-6, 125	22.25	21.63
1089B-3H-1, 120	15.5	21.64	Tie to	1089B-3H-6, 115	22.95	29.09
1089C-4H-1, 145	24.85	29.13	Tie to	1089C-4H-5, 50	29.9	34.18
1089B-4H-3, 115	27.95	34.25	Tie to	1089B-4H-6, 49	31.79	38.1
1089C-5H-1, 110	34	38.12	Tie to			

Note: Same as shipboard splice below 177-1089C-5H-1, 110 cm, but add 0.7 m to shipboard mcd.

Table T4. $\delta^{18}\text{O}$ and $\delta^{13}\text{C}$ of benthic and planktonic foraminifers and weight percent CaCO_3 at Site 1090 and piston core TTN057-6.

Site/Hole	Core	Section	Interval top (cm)	Interval bottom (cm)	Depth (mcd)	Age (ka)	$\delta^{18}\text{O}$ C. wuellerstorfi (‰)	$\delta^{13}\text{C}$ C. wuellerstorfi (‰)	$\delta^{18}\text{O}$ C. kullenbergi (‰)	$\delta^{13}\text{C}$ C. kullenbergi (‰)	$\delta^{18}\text{O}$ G. bulloides (‰)	$\delta^{13}\text{C}$ G. bulloides (‰)	$\delta^{18}\text{O}$ N. pachyderma (‰)	$\delta^{13}\text{C}$ N. pachyderma (‰)	CaCO_3 (wt%)	Lab
TTN057-6	PC4	IX	3	5	0.03	0.83			2.73	0.22	1.61	0.58	1.53	0.44	85.0	UF
TTN057-6	PC4	IX	6	8	0.06	1.66			2.75	0.08	1.30	0.04	1.39	0.44	81.0	UF
TTN057-6	PC4	IX	9	11	0.09	2.48	2.58	0.50	2.79	-0.01	1.78	0.61	1.35	0.75	86.4	UF
TTN057-6	PC4	IX	12	14	0.12	3.31			2.63	0.20	1.53	0.42	1.24	0.66	83.0	UF
TTN057-6	PC4	IX	15	17	0.15	4.14			2.76	0.30	1.47	0.03	1.38	0.58	85.0	UF
TTN057-6	PC4	IX	18	20	0.18	4.97			2.67	0.13	1.79	0.35	1.35	0.59	85.9	UF
TTN057-6	PC4	IX	21	23	0.21	5.79			2.71	0.19	1.83	0.40	1.30	0.55	87.6	UF
TTN057-6	PC4	IX	24	26	0.24	6.62			2.84	-0.21	1.29	-0.11	1.49	0.49	87.8	UF
TTN057-6	PC4	IX	27	29	0.27	7.45			2.75	-0.05	1.99	0.18	1.32	0.65	87.4	UF
TTN057-6	PC4	IX	30	32	0.30	8.28			3.06	-0.33	1.80	-0.06	1.44	0.46	81.5	UF
TTN057-6	PC4	IX	33	35	0.33	9.10			2.92	-0.34	2.03	-0.18	1.79	0.30	82.3	UF
TTN057-6	PC4	IX	36	38	0.36	9.93			2.95	-0.38	2.12	-0.26	1.63	0.09	84.4	UF
TTN057-6	PC4	IX	39	41	0.39	10.76	2.79	0.32	2.98	-0.20	2.05	0.15	1.71	0.42	85.7	UF
TTN057-6	PC4	IX	42	44	0.42	11.59			3.56	-0.64	2.00	-0.73	1.87	0.30	83.2	UF
TTN057-6	PC4	IX	45	47	0.45	12.41	3.59	0.22	3.74	-0.62	2.56	-0.17	2.15	0.10	85.2	UF
TTN057-6	PC4	IX	48	50	0.48	13.24	3.95	-0.34	3.69	-0.68	2.68	-0.18	1.97	-0.14	81.8	UF
TTN057-6	PC4	IX	51	53	0.51	14.07	4.09	-0.28	3.92	-0.91	2.34	-0.54	2.05	-0.04	82.3	UF
TTN057-6	PC4	IX	54	56	0.54	14.90	4.03	-0.03	3.92	-0.66	2.69	-0.45	2.39	-0.17	73.7	UF
TTN057-6	PC4	IX	57	59	0.57	15.74	3.59	0.16	3.92	-0.88	2.96	-0.19	2.41	-0.29	67.0	UF
TTN057-6	PC4	IX	60	62	0.60	16.58			4.38	-0.61	2.91	-0.48	2.80	-0.69	63.3	UF
TTN057-6	PC4	IX	63	65	0.63	17.42			4.23	-0.40	3.13	-0.36			59.9	UF
TTN057-6	PC4	IX	66	68	0.66	18.26					3.30	-0.03	2.77	-0.79	60.8	UF
TTN057-6	PC4	IX	69	71	0.69	19.10					3.09	-0.35	2.95	-0.66	61.3	UF
TTN057-6	PC4	IX	72	74	0.72	19.94			4.17	-0.99	3.08	-0.49			59.5	UF
TTN057-6	PC4	IX	75	77	0.75	20.78					3.00	0.07	2.95	-0.62	53.3	UF
TTN057-6	PC4	IX	80	82	0.78	21.62	4.03	-0.26			3.32	-0.43	2.64	-0.62	52.6	UF
TTN057-6	PC4	IX	81	83	0.81	22.46	4.13	-0.62			2.46	0.03			53.6	UF
TTN057-6	PC4	IX	84	86	0.84	23.30					3.29	0.26	3.00	-0.80	43.2	UF
TTN057-6	PC4	IX	87	89	0.87	24.15	4.21	-0.03			3.02	-0.53	2.52	-0.80	44.2	UF
TTN057-6	PC4	IX	90	92	0.90	24.99					2.80	0.09			43.1	UF
TTN057-6	PC4	IX	93	95	0.93	25.83	3.72	-0.13			2.76	0.09	2.76	-0.71	39.5	UF
TTN057-6	PC4	IX	96	98	0.96	26.67					2.10	-0.13			41.6	UF
TTN057-6	PC4	IX	99	101	0.99	27.51	3.00	0.16			2.17	0.18	2.52	-0.82	46.2	UF
TTN057-6	PC4	IX	102	104	1.02	28.35	4.15	-0.33			2.31	0.07	2.56	-0.91	46.8	UF
TTN057-6	PC4	VIII	0	2	1.03	28.74	4.01	-0.24			3.05	-0.38	2.50	-0.55		UF
TTN057-6	PC4	VIII	3	5	1.06	29.58					3.05	0.25	2.72	-0.41	51.5	UF
TTN057-6	PC4	VIII	6	8	1.09	30.42					3.15	0.59			52.3	UF
TTN057-6	PC4	VIII	9	11	1.12	31.26	3.87	-0.38			3.04	0.48	2.70	-0.54	61.7	UF
TTN057-6	PC4	VIII	12	14	1.15	32.10					2.86	0.13			65.8	UF
TTN057-6	PC4	VIII	15	17	1.18	32.94	3.97	-0.40			2.90	-0.02	2.61	-0.23	65.7	UF
TTN057-6	PC4	VIII	18	20	1.21	33.79	3.81	0.01			3.06	0.04			66.3	UF
TTN057-6	PC4	VIII	21	23	1.24	34.63	3.80	-0.17			3.13	0.27			70.6	UF
TTN057-6	PC4	VIII	24	26	1.27	35.47	3.83	0.03			2.97	-0.22	2.68	-0.08	73.4	UF
TTN057-6	PC4	VIII	27	29	1.30	36.31	3.71	-0.35			2.91	-0.08			75.6	UF
TTN057-6	PC4	VIII	39	41	1.42	39.67					3.01	0.18	2.76	-0.39	69.9	UF

Note: Only a portion of this table appears here. The entire table is available in [ASCII format](#).

Table T5. Isotope stages missing at Site 1090.

Depth (mcd)	Age (ka)	Missing marine isotopic stages
40.37	1458–1476	48
44.37	1835–1867	66–67
50.79	2256–2295	86–88
51.84	2361–2391	90/91
53.68	2543–2577	101
56.08	2720–2820	110–114

Table T6. $\delta^{18}\text{O}$ and $\delta^{13}\text{C}$ of the planktonic foraminifer *N. pachyderma* (sinistral) at Site 1093.

Site	Hole	Core	Section	Interval top (cm)	Interval bottom (cm)	Depth (mcd)	$\delta^{18}\text{O}$ (‰)	$\delta^{13}\text{C}$ (‰)	Lab
1093	A	1	1	0	2	0.00	2.56	1.16	SIO
1093	A	1	1	10	12	0.10	2.68	1.28	SIO
1093	A	1	1	20	22	0.20			SIO
1093	A	1	1	30	32	0.30	2.66	1.25	SIO
1093	A	1	1	40	42	0.40	2.58	1.21	SIO
1093	A	1	1	50	52	0.50	2.67	1.20	SIO
1093	A	1	1	60	62	0.60	2.53	1.24	SIO
1093	A	1	1	70	72	0.70	2.52	1.20	SIO
1093	A	1	1	80	82	0.80	2.68	1.11	SIO
1093	A	1	1	90	92	0.90	2.50	1.10	SIO
1093	A	1	1	100	102	1.00	2.51	1.16	SIO
1093	A	1	1	110	112	1.10	2.34	1.02	SIO
1093	A	1	1	120	122	1.20	2.47	1.16	SIO
1093	A	1	1	130	132	1.30	2.47	1.15	SIO
1093	A	1	1	140	142	1.40	2.57	1.23	SIO
1093	A	1	2	0	2	1.50	2.36	1.10	SIO
1093	A	1	2	10	12	1.60	2.59	0.93	SIO
1093	A	1	2	20	22	1.70	2.56	0.99	SIO
1093	A	1	2	30	32	1.80	2.41	1.09	SIO
1093	A	1	2	40	42	1.90	2.45	1.00	SIO
1093	A	1	2	50	52	2.00	2.48	0.93	SIO
1093	A	1	2	60	62	2.10	2.51	1.05	SIO
1093	A	1	2	70	73	2.20	2.47	0.86	SIO
1093	A	1	2	80	83	2.30	2.35	1.04	SIO
1093	A	1	2	90	92	2.40	2.74	1.07	SIO
1093	A	1	2	100	102	2.50	2.63	0.82	SIO
1093	A	1	2	110	112	2.60	2.50	0.83	SIO
1093	A	1	2	120	122	2.70	2.39	0.87	SIO
1093	A	1	2	130	132	2.80	2.52	0.81	SIO
1093	A	1	2	140	142	2.90	2.67	0.82	SIO
1093	A	1	3	0	2	3.00	2.62	1.03	SIO
1093	A	1	3	10	12	3.10	2.53	0.79	SIO
1093	A	1	3	20	22	3.20	2.61	0.83	SIO
1093	A	1	3	30	32	3.30	2.76	0.85	SIO
1093	A	1	3	39	41	3.39	2.76	0.85	SIO
1093	A	1	3	50	52	3.50	2.39	0.06	SIO
1093	A	1	3	60	62	3.60	2.56	0.90	SIO
1093	A	1	3	67	69	3.67	2.46	0.46	SIO
1093	A	1	3	80	82	3.80	2.54	0.81	SIO
1093	A	1	3	90	92	3.90	2.48	0.83	SIO
1093	A	1	3	100	102	4.00	2.53	0.79	SIO
1093	A	1	3	110	112	4.10	2.60	0.55	SIO
1093	A	1	3	120	122	4.20	2.72	0.64	SIO
1093	A	1	3	130	132	4.30	2.87	0.70	SIO
1093	A	1	3	140	142	4.40			SIO
1093	A	1	4	0	2	4.50	2.87	0.71	SIO
1093	A	1	4	10	12	4.60	2.90	0.84	SIO
1093	A	1	4	20	22	4.70	2.86	0.71	SIO
1093	A	1	4	30	32	4.80	2.83	0.65	SIO
1093	A	1	4	40	42	4.90	2.90	0.66	SIO
1093	A	1	4	50	52	5.00	2.84	0.69	SIO
1093	A	1	4	60	62	5.10	3.00	0.73	SIO
1093	A	1	4	70	72	5.20	2.98	0.57	SIO
1093	A	1	4	77	79	5.27	2.95	0.65	SIO
1093	A	1	4	90	92	5.40			SIO
1093	A	1	4	100	102	5.50	2.63	0.46	SIO
1093	A	1	4	110	112	5.60	2.79	0.61	SIO
1093	A	1	4	120	122	5.70			SIO
1093	A	1	4	130	132	5.80	2.87	0.55	SIO
1093	A	1	4	140	142	5.90	2.79	0.35	SIO
1093	A	1	5	0	2	6.00	2.67	0.52	SIO
1093	A	1	5	10	12	6.10	2.83	0.82	SIO
1093	A	1	5	20	22	6.20	2.76	0.63	SIO
1093	A	1	5	30	32	6.30	2.66	0.69	SIO

Note: Only a portion of this table appears here. The entire table is available in [ASCII format](#).

Table T7. $\delta^{18}\text{O}$ and $\delta^{13}\text{C}$ of the planktonic foraminifer *Neogloboquadrina pachyderma* (sinistral), Site 1094.

Site	Hole	Core	Section	Interval top (cm)	Interval bottom (cm)	Depth (mcd)	Age (ka)	$\delta^{18}\text{O}$ (‰)	$\delta^{13}\text{C}$ (‰)	Lab
1094	A	1	1	0	2	0.00	0.21	3.24	0.76	UF
1094	A	1	1	5	7	0.05	0.29			UF
1094	A	1	1	10	12	0.10	0.38			UF
1094	A	1	1	15	17	0.15	0.46			UF
1094	A	1	1	20	22	0.20	0.55			UF
1094	A	1	1	25	27	0.25	0.63			UF
1094	A	1	1	30	32	0.30	0.72			UF
1094	A	1	1	35	37	0.35	0.80			UF
1094	A	1	1	40	42	0.40	0.89	3.01	0.69	UF
1094	A	1	1	45	47	0.45	0.97			UF
1094	A	1	1	50	52	0.50	1.06	3.20	0.62	UF
1094	A	1	1	55	57	0.55	1.14	3.08	0.83	UF
1094	A	1	1	60	62	0.60	1.23	3.52	1.07	UF
1094	A	1	1	65	67	0.65	1.31	3.20	1.04	UF
1094	A	1	1	70	72	0.70	1.40			UF
1094	A	1	1	75	77	0.75	1.48			UF
1094	A	1	1	80	82	0.80	1.57	3.22	0.88	UF
1094	A	1	1	85	87	0.85	1.65	2.97	0.74	UF
1094	A	1	1	90	92	0.90	1.73			UF
1094	A	1	1	95	97	0.95	1.82			UF
1094	A	1	1	100	102	1.00	1.90			UF
1094	A	1	1	105	107	1.05	1.99			UF
1094	A	1	1	110	112	1.10	2.07	3.06	0.92	UF
1094	A	1	1	115	117	1.15	2.16			UF
1094	A	1	1	120	122	1.20	2.24	3.10	1.00	UF
1094	A	1	1	125	127	1.25	2.33	3.16	1.03	UF
1094	A	1	1	130	132	1.30	2.41			UF
1094	A	1	1	135	137	1.35	2.50	2.96	0.62	UF
1094	A	1	1	140	142	1.40	2.58	3.28	0.73	UF
1094	A	1	2	0	2	1.50	2.75			UF
1094	A	1	2	5	7	1.55	2.84			UF
1094	A	1	2	10	12	1.60	2.92	3.48	0.95	UF
1094	A	1	2	15	17	1.65	3.00			UF
1094	A	1	2	20	22	1.70	3.09			UF
1094	A	1	2	25	27	1.75	3.17			UF
1094	A	1	2	30	32	1.80	3.26			UF
1094	A	1	2	35	37	1.85	3.34			UF
1094	A	1	2	40	42	1.90	3.43			UF
1094	A	1	2	45	47	1.95	3.51			UF
1094	A	1	2	50	52	2.00	3.60			UF
1094	A	1	2	55	57	2.05	3.68			UF
1094	A	1	2	60	62	2.10	3.77			UF
1094	A	1	2	65	67	2.15	3.85			UF
1094	A	1	2	70	72	2.20	3.94	3.37	0.76	UF
1094	A	1	2	75	77	2.25	4.02			UF
1094	A	1	2	80	82	2.30	4.11	3.07	0.71	UF
1094	A	1	2	85	87	2.35	4.19	3.15	0.65	UF
1094	A	1	2	90	92	2.40	4.28	3.01	0.60	UF
1094	A	1	2	95	97	2.45	4.36	3.11	0.71	UF
1094	A	1	2	100	102	2.50	4.44	3.05	0.68	UF
1094	A	1	2	105	107	2.55	4.53	3.03	0.65	UF
1094	C	1	2	80	82	2.58	4.58	3.32	0.66	UF
1094	C	1	2	85	87	2.63	4.66			UF
1094	C	1	2	90	92	2.68	4.75			UF
1094	C	1	2	95	97	2.73	4.83			UF
1094	C	1	2	100	102	2.78	4.92	3.03	0.49	UF
1094	C	1	2	105	107	2.83	5.00	2.86	0.58	UF
1094	C	1	2	110	112	2.88	5.09	2.86	0.53	UF
1094	C	1	2	115	117	2.93	5.17	3.06	0.52	UF
1094	C	1	2	120	122	2.98	5.26	3.15	0.54	UF
1094	C	1	2	125	127	3.03	5.34			UF
1094	C	1	2	130	132	3.08	5.43	3.49	1.05	UF
1094	C	1	2	135	137	3.13	5.51	3.45	0.55	UF

Note: Only a portion of this table appears here. The entire table is available in [ASCII format](#).